

Equation-Free Coarse Control of Distributed Parameter Systems via Local Neural Operators

Gianluca Fabiani¹, Constantinos Siettos², and Ioannis G. Kevrekidis³

Abstract—The control of high-dimensional distributed parameter systems (DPS) remains a challenge when explicit coarse-grained equations are unavailable. Classical equation-free (EF) approaches rely on fine-scale simulators treated as black-box timesteppers. However, repeated simulations for steady-state computation, linearization, and control design are often computationally prohibitive, or the microscopic timestep may not even be available, leaving us with data as the only resource. We propose a data-driven alternative that uses *local neural operators*, trained on spatiotemporal microscopic/mesoscopic data, to obtain efficient short-time solution operators. These surrogates are employed within Krylov subspace methods to compute coarse steady and unsteady-states, while also providing Jacobian information in a matrix-free manner. Krylov–Arnoldi iterations then approximate the dominant eigenspectrum, yielding reduced models that capture the open-loop slow dynamics without explicit Jacobian assembly. Both discrete-time Linear Quadratic Regulator (dLQR) and pole-placement (PP) controllers are based on this reduced system and lifted back to the full nonlinear dynamics, thereby closing the feedback loop.

I. INTRODUCTION

Modelling and, importantly controlling, high-dimensional, multiscale complex systems remains a major challenge across engineering and science [1], [2], [3]. Many such systems are governed by complex interactions among large numbers of agents or particles, often leading to emergent behavior that is difficult to predict and regulate, including catastrophic shifts or major irreversible changes in dominant mesoscopic or macroscopic spatio-temporal patterns [4]. These systems frequently exhibit multistability, with multiple possible steady-states – some stable, others unstable – among which certain states may be desirable to reach or maintain through control interventions [5], [6], [7].

*G.F. and I.G.K. work was partially supported by the Department of Energy under Grant No. DE-SC0024162, as well as partial support by the National Science Foundation under Grants No. CPS2223987 and FDT2436738. C.S. acknowledges partial support by the PNRR MUR projects PE0000013-Future Artificial Intelligence Research-FAIR & CN0000013 CN HPC - National Centre for HPC, Big Data and Quantum Computing, Gruppo Nazionale Calcolo Scientifico-Istituto Nazionale di Alta Matematica (GNCS-INdAM)

¹G. Fabiani is with Hopkins Extreme Materials Institute and Department of Chemical and Biomolecular Engineering, Johns Hopkins University, 3400 North Charles Street, Baltimore, 21218 MD, USA gfabian2@jh.edu

²C. Siettos with the Dipartimento di Matematica e Applicazioni “Renato Caccioppoli”, Università degli studi di Napoli Federico II, Via Vicinale Cupa Cintia, 26, 80126 Naples NA, Italy constantinos.siettos@unina.it

³I.G. Kevrekidis with Department of Chemical and Biomolecular Engineering, Department of Applied Mathematics and Statistics, and School of Medicine’s Department of Urology, Johns Hopkins University, 3400 North Charles Street, Baltimore, 21218 MD, USA yannisk@jhu.edu

The control of high-dimensional DPS remains especially challenging when explicit coarse-grained equations are unavailable. In such cases, classical control design tools cannot be directly applied, as they typically rely on low-dimensional state-space or PDE-based representations [8], [9]. This lack of tractable models hinders the systematic design of observers, stabilizing controllers, and feedback laws. Developing frameworks that bypass or replace explicit macroscopic models is therefore essential for enabling principled, data-driven control in these settings. One of such frameworks is the *Equation-Free* (EF) approach [1], [10], [11], introduced in the early 2000s. It provides a systematic way to connect microscopic or high-fidelity simulations with system-level tasks for emergent macroscopic dynamics, while avoiding the explicit derivation of closed-form surrogate equations – hence the term equation-free, in analogy to matrix-free linear algebra methods. Assuming access to microscopic simulators (such as Monte Carlo, Lattice–Boltzmann, or Molecular Dynamics), and under suitable process conditions, EF constructs coarse timesteppers to evolve macroscopic observables directly. These timesteppers can then be embedded in computational superstructures for tasks such as stability and bifurcation analysis, as well as for control design, relying on well-established numerical methods including contraction mappings (e.g., the Recursive Projection Method), matrix-free Krylov solvers (e.g., Conjugate Gradient (CG); Generalized Minimal Residual (GMRES)), and eigensolvers such as Arnoldi algorithm [12], [13].

However, a limitation of the classical EF framework is that its surrogates are constructed *on demand*, requiring repeated calls to the underlying microscopic simulator. This repeated use can be computationally prohibitive, and in many applications the microscopic simulator may not even be available, leaving observational data as the only viable resource. This shifts the focus toward learning surrogate operators *directly from measurements*, often under partial-information or sparse-data regimes.

In this context, a longstanding goal is to learn effective models or reconstructing operators that describe the system’s evolution. Two complementary approaches exist: (i) analytical approaches – mean-field limits, Fokker–Planck equations, and moment closures – deriving macroscopic PDEs from microscopic physics through kinetic or statistical mechanics [14]; and (ii) more recent data-driven methods, learning operators directly from high-fidelity simulations [15], [16], [17], [18], [19], [20], [3]. Classical analytical methods can provide closed-form approximations, but are difficult to derive analytically [21] and typically rely on assumptions

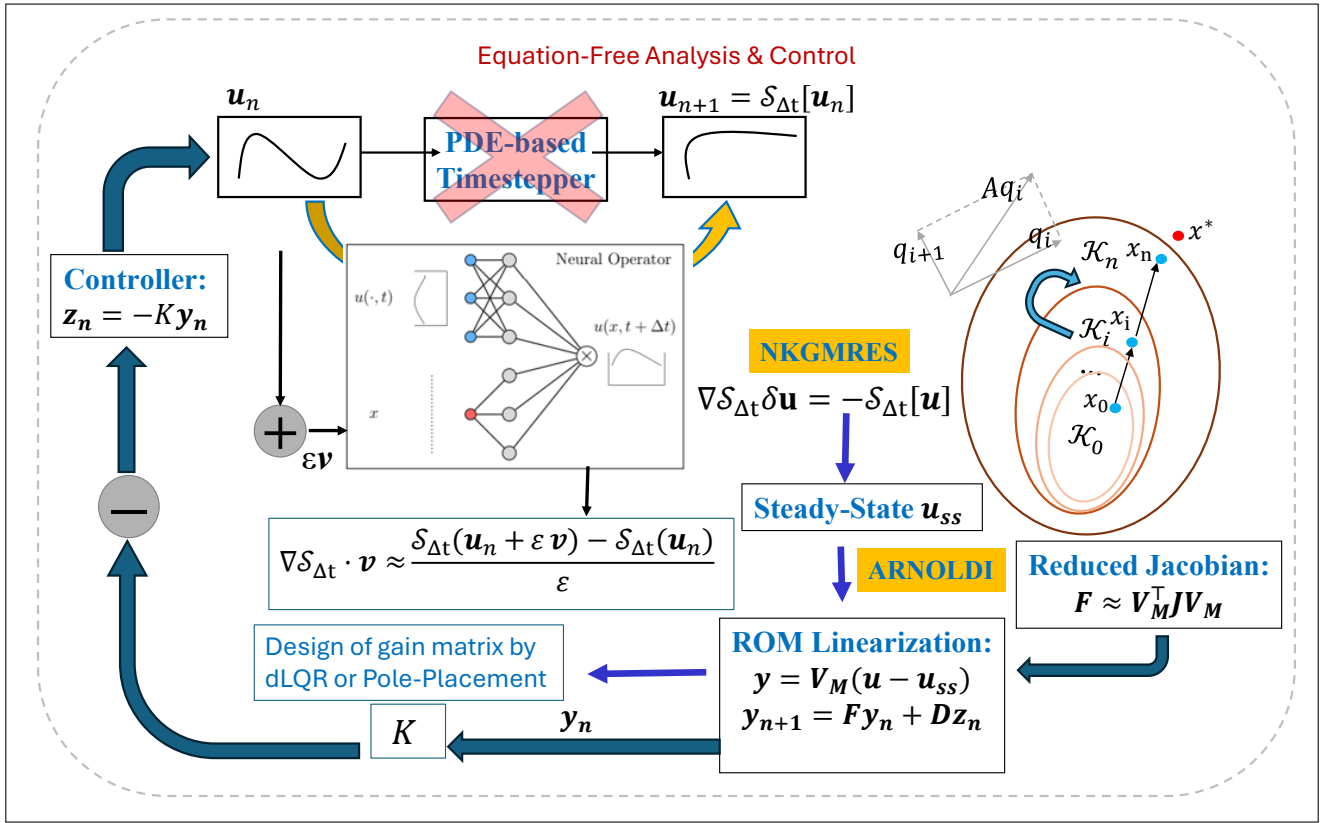


Fig. 1. Schematic of the equation-free control pipeline via Neural Operators (NOs). An NO, trained on spatiotemporal data, replaces the unavailable traditional PDE-based time-stepper. This surrogate enables matrix-free computation of coarse steady-states (via Newton-Krylov GMRES) and the dominant eigenmodes of the linearization (via Arnoldi iteration). The resulting low-dimensional model is used to design a controller (here, dLQR or pole-placement), which is then implemented in closed loop by feeding control inputs back to the NO-timestepper.

that may bias the resulting models, often yielding qualitative rather than fully quantitative accuracy [3]. On the other hand, data-driven methods relax strong *a priori* assumptions but introduce their own challenges: sparse or partial observations; the “curse of dimensionality”; strong nonlinearities and stiffness; multiple, separated time scales; and both epistemic (model) and aleatoric (measurement) uncertainty – all of which exacerbate ill-posedness and identifiability. On top of these difficulties, algorithmic choice becomes critical. Common tools in machine learning – standard artificial neural networks (ANNs), Gaussian processes (GPs) – are designed for finite-dimensional regression, i.e., functions $f: \mathbb{R}^n \rightarrow \mathbb{R}^m$. By contrast, model discovery for multiscale systems often requires learning operators $\mathcal{G}: \mathcal{U} \rightarrow \mathcal{V}$ that map between infinite-dimensional function spaces (e.g., L^2 or Sobolev spaces), for example, the infinite-dimensional nature of models such as PDEs. Neural Operators (NOs) [18], [22] were introduced to address this gap, yielding surrogates that can generalize across input functions, possibly different resolutions, boundary conditions, and even additional bifurcation parameters. NO-learning architectures have proliferated in recent years. Representative frameworks include DeepONet [18], Fourier NOs (FNOs) [22], Graph NOs (GNOs) [23], Spectral NOs (SNOs) [24], and more recently Random Projection-based Operator Networks (Ran-

dONets) [25]. When working with spatio-temporal data, there are two main types of operators that one may seek to learn. One is the continuous-time RHS governing operator [16], [25], representing the system’s derivative mapping, which allows flexible time-integration, interpretability, and applicability to changing domains. The second is the solution operator (a.k.a. timestepper), mapping an initial state to a future state over finite time, embedding boundary conditions naturally and requiring fewer assumptions about the system dynamics [22], [26]. Both approaches face challenges for long-time predictions, particularly in systems with chaotic behavior, multiple basins of attraction, or high-frequency modes that are difficult to resolve due to the spectral bias of NOs [27], [28]. To mitigate this, local-in-time and sometimes local-in-space operators are preferable, trained on short-time snapshots and augmented to maximize data efficiency [26], [28], [27].

NOs have so far been used mainly to accelerate brute-force simulations, providing fast surrogates once trained. This enables rapid predictions and the generation of large ensembles of trajectories, supporting tasks such as Monte Carlo-based uncertainty quantification or rare-event analysis [3]. In recent work [26], we introduced Local NOs as an equation-free building block, coupled with matrix-free Krylov methods [12], [13], to extend their role beyond trajectory generation toward coarse-grained bifurcation analysis.

Building on this foundation, and inspired by related equation-free coarse control strategies [29], [5], [30], [31], [6], we now broaden the scope of NO-timesteppers to coarse feedback control of dissipative spatially distributed processes.

Our framework follows a two-step coarse controller design. First, fine-scale simulations are processed through the coarse timestepper to identify the target coarse stationary state, approximate the subspace spanned by the dominant slow modes in its neighborhood, and characterize the action of the coarse linearization on this subspace. For this task, we employ Newton–Krylov iterations in combination with the coarse timestepper to construct coarse fixed-point solvers and eigensolvers. This procedure yields an approximate reduced-order coarse model suitable for feedback design.

To enable feedback stabilization, spatially localized actuators are introduced, and their effect is quantified by perturbing the timestepper and recording directional derivatives. This allows us to construct reduced discrete-time input–output models coupling actuator actions with the unstable modes. On these reduced models, we design discrete-time controllers – both pole-placement (PP) controllers and optimal strategies based on the discrete-time Linear Quadratic Regulator (dLQR) [5], [30], [32]. The resulting control actions are then lifted and applied directly to the original nonlinear timestepper, thereby stabilizing unstable coarse stationary states. Krylov subspace techniques play a central role in this pipeline, enabling the computation of coarse fixed points and matrix-free Jacobian information around equilibria, even for large-scale systems. Fig. 1 provides a schematic illustration of the EF Analysis and Control framework via local NOs. We demonstrate the methodology on one representative problem: the parabolic Liouville-Bratu equation [33]. We compare results obtained with a NO-timestepper against those obtained with a finite-difference PDE solver. The data-driven and physics-based approaches produce consistent stabilizing feedback laws.

II. PRELIMINARIES

A. Problem Statement

Our focus is on learning data-driven approximations of the *solution operator* (or “time-stepper”) of PDEs using NOs. Let’s consider the continuous-time *RHS governing operator* $\mathcal{L} : \mathbf{U} \rightarrow \mathbf{U}$ of a PDE:

$$\begin{aligned} \frac{\partial u(\mathbf{x}, t)}{\partial t} &= \mathcal{L}[u](\mathbf{x}, t), & \mathbf{x} \in \Omega, & \quad t \in [0, T], \\ \mathcal{B}[u](\mathbf{x}, t) &= g(\mathbf{x}, t), & \mathbf{x} \in \partial\Omega, \end{aligned} \quad (1)$$

where \mathcal{B} and g denote the boundary conditions, $u : \Omega \subseteq \mathbb{R}^d \times [0, T] \rightarrow \mathbb{R}$ is the unknown solution of the PDE, and \mathbf{U} is an appropriate functional space, such as Sobolev space $H^2(\Omega)$. Given a generic function state $u(\cdot, t)$ at time t , the solution operator $\mathcal{S}_{\Delta t}$ outputs a new function $v : \Omega \rightarrow \mathbb{R}$ that correspond to the future function state $u(\cdot, t + \Delta t) : \Omega \rightarrow \mathbb{R}$ after a time horizon Δt :

$$v(\mathbf{x}) := u(\mathbf{x}, t + \Delta t) = \mathcal{S}_{\Delta t}[u(\cdot, t)](\mathbf{x}), \quad \mathcal{S}_{\Delta t} : \mathbf{U} \rightarrow \mathbf{U}. \quad (2)$$

Note that boundary conditions are implicitly included in $\mathcal{S}_{\Delta t}$.

The trained time-stepper provides a global-in-space and discrete-time surrogate of the solutions of the PDE, mapping input functions (e.g., initial conditions) to system states at prescribed later times. Once learned, it can be applied iteratively for system-level tasks, or combined with projective integration steps as in [26]. In the standard multiscale EF framework, the timestepper is constructed *on demand* whenever needed and discarded afterward. By contrast, in our EF–Local NO framework, the same neural timestepper, once trained, is reused across different initial conditions.

B. Neural Operators à la Chen and Chen

We briefly summarize the general framework of Chen and Chen work [34], which underlies both DeepONets and RandONets. While the theoretical goal is to learn operators on infinite-dimensional spaces, practical learning requires discretization. A standard approach is to represent functions by their values on a finite set of sensor locations $\mathbf{x}_1, \dots, \mathbf{x}_m \in \mathbf{X} \subseteq \mathbb{R}^d$. These samples $u(\mathbf{x}_j)$ serve as inputs to the network. Consider approximating an operator \mathcal{F} acting on s samples of functions $u_q \in \mathbf{U}$, $q = 1, \dots, s$, discretized at m locations $\mathbf{x}_1, \dots, \mathbf{x}_m \in \mathbf{K}_1$. The q -th input vector

$$\mathbf{U}_q = (u_q(\mathbf{x}_1), \dots, u_q(\mathbf{x}_m)) \in \mathbb{R}^{m \times 1} \quad (3)$$

is processed by a *branch* network, a single (or multi) hidden layer ANN with M neurons, activation ϕ^{br} , weights $\alpha_{ij}^{br} \in \mathbb{R}$, and biases $\beta_i^{br} \in \mathbb{R}$. The *trunk* network, with N neurons, activation ϕ^{tr} , weights $\alpha_k^{tr} \in \mathbb{R}^d$, and biases β_k^{tr} , processes the target location $\mathbf{x}_j \in \mathbf{K}_2 \subset \mathbb{R}^{1 \times d}$. The hidden layer values of the branch and trunk nets are represented by $\mathbf{B} = (B_1, \dots, B_M) \in \mathbb{R}^{M \times 1}$ and $\mathbf{T} = (T_1, \dots, T_N) \in \mathbb{R}^{1 \times N}$, respectively:

$$\begin{aligned} B_i(\mathbf{U}_q) &= \phi^{br} \left(\sum_{j=1}^m \alpha_{ij}^{br} u_q(\mathbf{x}_j) + \beta_i^{br} \right), & i = 1, \dots, M, \\ T_k(\mathbf{x}_j) &= \phi^{tr} (\mathbf{x}_j \cdot \alpha_k^{tr} + \beta_k^{tr}), & k = 1, \dots, N. \end{aligned} \quad (4)$$

The network output is then the *weighted inner product* of the branch and trunk outputs:

$$\mathcal{F}[u](\mathbf{y}) \approx \sum_{k=1}^N \sum_{i=1}^M w_{ki} B_i(\mathbf{U}) T_k(\mathbf{y}) = \mathbf{T} \mathbf{W} \mathbf{B} = \langle \mathbf{T}, \mathbf{B} \rangle_W, \quad (5)$$

where the matrix $\mathbf{W} \in \mathbb{R}^{N \times M}$ contains the weights w_{ki} .

While Chen and Chen originally used shallow networks, DeepONets extend the framework to deeper architectures or other types of ANNs. Training these large networks is computationally demanding and typically requires GPUs. To address this, we employ RandONets [25], which provide efficient randomized embeddings; a brief description follows.

C. RandONets

Despite their theoretical universality [35], [34], standard deep ANNs and NOs often exhibit slow convergence, over-parameterization, and high computational cost, limiting their accuracy in high-precision scientific computations [36], [37], [38], [39].

RandONets [25] attempt to address these issues by replacing fully trainable hidden layers with fixed randomized embeddings, leveraging random projections and the Johnson–Lindenstrauss lemma [40] to exploit the universal approximation power of random features [41], [42], [43], [44]. In particular, the trunk network weights $(\alpha_k^{tr}, \beta_k^{tr})$, which usually process low-dimensional spatial locations, are sampled i.i.d. from continuous distributions, e.g., parsimonious or optimized uniform distributions as in [45], [46], with sigmoidal activation functions $\sigma = 1/(1 + \exp(-x))$ and $\alpha_k^{tr} \sim \mathcal{U}[-a_U, a_U]$, where a_U is the bound of the uniform distribution, i.e. an hyper-parameter that can be tuned. Trunk biases β_k^{tr} are determined from random sampled centers \mathbf{c}_k^{tr} (inflection points) of the sigmoids within the domain of interest Ω , defined by $-\alpha_k^{tr} \cdot \mathbf{c}_k^{tr} = \beta_k^{tr}$, with $\mathbf{c}_k^{tr} \sim \mathcal{U}[\Omega]$ (see [45], [46], [20], [25] for details).

The branch network, which processes very high-dimensional function features, requires more sophisticated random embeddings. Due to their simplicity and analytical connection to reproducing kernel Hilbert space (RKHS) approximations, we employ nonlinear random Fourier feature networks (RFFN) [42], [43]:

$$\mathbf{B} = \sqrt{\frac{2}{M}} [\cos(\alpha_1^{br} \cdot \mathbf{U} + \beta_1^{br}), \dots, \cos(\alpha_M^{br} \cdot \mathbf{U} + \beta_M^{br})], \quad (6)$$

where branch weights α_k^{br} are zero-mean Gaussian distributed $\alpha_k^{br} \sim \mathcal{N}(0, \varepsilon)$ and biases $\beta_k^{br} \sim \mathcal{U}[0, 2\pi]$, corresponding to RFFN approximations of Gaussian-based RKHS, where the hyper-parameter ε is tunable.

The only remaining unknown, the network output weights W in Eq. (5), are then determined via a *bilinear matrix equation* using standard least-squares, e.g., by computing two decoupled pseudo-inverses for the branch and trunk matrices separately.

This design converts the original non-convex, gradient-based training into a convex linear least-squares one. While potentially high-dimensional and ill-conditioned, the bilinear system can be efficiently solved using Moore–Penrose pseudoinverse, Tikhonov regularization, QR decomposition, or complete orthogonal decomposition [25].

D. Equation-Free system-level computations via local NOs: fixed-points and stability

Directly approximating long-time prediction, i.e. large Δt , is challenging, as the operator become stiff and prone to instabilities in high-frequency modes due to spectral bias. It is often more efficient to learn local-in-time solution operators $\mathcal{S}_{\Delta t}$ and apply them autoregressively, taking advantage of the semigroup property, to reconstruct long time horizon T :

$$u(\mathbf{x}, T) = \mathcal{S}_T[u] = \underbrace{\mathcal{S}_{\Delta t} \circ \mathcal{S}_{\Delta t} \circ \dots \circ \mathcal{S}_{\Delta t}}_{\frac{T}{\Delta t} \text{ times}}[u]. \quad (7)$$

This can suffer from error accumulation, especially for high-frequency modes. Instead, steady-states can be obtained directly as fixed points of the short-time solution operator:

$$u^* = \mathcal{S}_T[u^*], \quad \psi(u) = u - \mathcal{S}_T[u]. \quad (8)$$

Newton’s method computes zeros of ψ :

$$\nabla \psi(u^{(k)}) \delta^{(k)} = -\psi(u^{(k)}), \quad \delta^{(k)} = u^{(k+1)} - u^{(k)}. \quad (9)$$

E. Krylov Subspace Methods

Krylov methods are among the top ten algorithms of the 20th century for a reason: they solve large linear systems ($Ax = b$) efficiently using only matrix-vector products. Starting from $x^{(0)}$ with initial residual $r^{(0)} = b - Ax^{(0)}$, Krylov methods build iteratively an increasing family of subspaces \mathcal{K}_i and a sequence of approximations x_i :

$$x_1, x_2, \dots, x_n \in x_0 + \mathcal{K}_i(A, r_0), \quad i = 1, \dots, n, \quad (10)$$

where the *Krylov subspace* is defined as

$$\mathcal{K}_n = \text{span}\{r_0, Ar_0, A^2r_0, \dots, A^{n-1}r_0\}. \quad (11)$$

In GMRES the approximation x_i is chosen to minimize the residual norm over that affine space:

$$x_i = \underset{x \in x_0 + \mathcal{K}_i(A, r_0)}{\text{argmin}} \|b - Ax\|_2. \quad (12)$$

Convergence depends on the spectral distribution of A ; preconditioning and restarting are commonly used in practice. For large nonlinear systems $\psi(u) = 0$, Newton–Krylov methods solve the linearized system $J^{(k)} \delta = -\psi(u^{(k)})$ with $J^{(k)} = \nabla \psi(u^{(k)})$. The Jacobian-vector products needed in this process can be cheaply obtained via finite difference approximation of the directional derivative:

$$\nabla \psi(u^{(k)}) r_0 \approx \frac{\psi(u^{(k)} + \varepsilon r_0) - \psi(u^{(k)})}{\varepsilon}. \quad (13)$$

Around the obtained steady-state, we compute approximate critical eigenvalues and eigenvectors via the Krylov–Arnoldi algorithm. Arnoldi builds an orthonormal basis Q_m of the Krylov subspace \mathcal{K}_m . The Jacobian projected onto this basis yields an upper Hessenberg matrix $H_m = Q_m^T J Q_m$. The Ritz values (eigenvalues of H_m) approximate the critical eigenvalues of the full Jacobian, thus providing stability information [13]. The associated Ritz vectors $Q_m v$ span a low-dimensional subspace \mathcal{P} approximating the dominant eigenspace of the Jacobian, which can be used to analyze and locally linearize the system [32].

III. METHODS

In this section, we outline the construction of linear discrete-time controllers for spatially distributed processes using NO-timestepper surrogates. The procedure consists of two stages. First, the surrogate is employed-together with Newton-Krylov GMRES and Arnoldi iterations to identify the dominant coarse dynamics, approximate coarse fixed points, and estimate the associated slow Jacobian. Second, based on this reduced linearized model, we design discrete-time controllers using either pole placement or optimal strategies such as dLQR.

A. Controlled Neural Operator Timestepper

The dynamics of the spatially distributed process are represented by a NO-timestepper $\mathcal{S}_{\Delta t}$, which advances the state u_n by one step of size Δt . We introduce the (open-loop) controlled NO-timestepper

$$u_{n+1} = \Phi(u_n, z_n) = \mathcal{S}_{\Delta t}(u_n) + G(u_n, z_n), \quad (14)$$

where $u_n = u(\cdot, t)$, $u_{n+1} = u(\cdot, t + \Delta t)$, and $z_n \in \mathbb{R}^k$ denotes the control input. The actuator contribution $G(u_n, z_n)$ satisfies $G(u_n, 0) \equiv 0$ and represents the correction induced by the applied controls. In the ideal setting, Φ constitutes the fully controlled one-step operator, combining the autonomous dynamics $\mathcal{S}_{\Delta t}$ with the actuator effects, and requires training with data that include controlled trajectories. The subsequent coarse linearization and controller design are then performed directly on this operator. Later, in Section IV-A, we address the more practical case in which such controlled data are not available, and discuss how controllers can be designed using only the autonomous NO timestepper.

B. Obtaining the Coarse Slow Linearization

The system identification stage aims to determine the target coarse stationary state u_{ss} and a linearized model of the slow dynamics around it. This is accomplished by first identifying the autonomous slow behavior and then evaluating the effect of actuators on the system.

Open-loop stationary states are located as the solution to $u_{ss} = \mathcal{S}_{\Delta t}(u_{ss})$ using a Newton-Krylov-GMRES iteration wrapped around the NO timestepper. In this framework, the Jacobian-vector products required by the GMRES linear solver, they are computed in a matrix-free manner, without explicitly constructing the full Jacobian matrix. The action of the Jacobian of the timestepper at the fixed point, $J = \partial \mathcal{S}_{\Delta t} / \partial x|_{(u_{ss})}$, in selected directions is approximated through directional finite differences approximation of the directional derivative:

$$Jv \approx \frac{\mathcal{S}_{\Delta t}(u_{ss} + \varepsilon v) - \mathcal{S}_{\Delta t}(u_{ss})}{\varepsilon}, \quad (15)$$

where ε is a small perturbation parameter and v is an arbitrary vector. The Arnoldi algorithm provides an orthonormal basis $V_M \in \mathbb{R}^{N \times M}$ for the slow subspace \mathcal{P} , and a low-dimensional representation of the Jacobian's action in this subspace, $F = V_M^\top J V_M \in \mathbb{R}^{M \times M}$.

This yields a low-dimensional linearization of the slow subsystem. Let $y_n \in \mathbb{R}^M$ be the coordinates of the deviation from the stationary state within the slow subspace, defined by the projection:

$$y_n = V_M^\top (u_n - u_{ss}). \quad (16)$$

The dynamics of these slow coordinates are approximated by the uncontrolled discrete-time system:

$$y_{n+1} = F y_n, \quad y_n \in \mathbb{R}^M, \quad (17)$$

Actuator Effects. Once the stationary state is identified, the effect of actuators *in the slow subspace* is estimated by perturbing the system and evaluating derivatives with

respect to the control inputs. Combining the autonomous linearization with these derivatives yields the low-dimensional approximate open-loop discrete-time system:

$$y_{n+1} = F y_n + D z_n, \quad (18)$$

where $z_n \in \mathbb{R}^k$ represents the control inputs, and $D \in \mathbb{R}^{M \times k}$ approximates the actuator influence on the slow modes. The matrix D is constructed as

$$D = V_F [V_M^\top V_M]^{-1} V_M^\top H, \quad (19)$$

where $V_F \in \mathbb{R}^{M \times M}$ contains the corresponding eigenvectors of F (ordered consistently with the eigenvalues in V), and $H \in \mathbb{R}^{N \times k}$ contains the numerically computed partial derivatives of \mathcal{S}_T with respect to the k control actuators.

C. Feedback control design

Linear feedback controllers are designed to stabilize (or improve the stability characteristics) of the target stationary state exploiting the low-dimensional model. The goal is to design a feedback gain matrix $K \in \mathbb{R}^{k \times M}$ such that the control law $z_n = -K y_n$ stabilizes the target stationary state by shaping the dynamics of the reduced slow subsystem:

$$y_{n+1} = (F - DK) y_n. \quad (20)$$

Here, we employ two alternative methodologies to compute a gain matrix K .

a) *Pole Placement:* This approach directly assigns the eigenvalues μ_i of the closed-loop matrix $(F - DK)$ to desired locations inside the unit circle. The gain matrix K is the solution to the eigenvalue assignment problem. This provides direct control over the transient response of the slow modes. In practice, we compute K using MATLAB's `place` function from the Control Toolbox.

b) *Discrete-Time Linear Quadratic Regulator (dLQR):* The dLQR approach computes the optimal gain matrix K by minimizing the quadratic cost function:

$$\mathcal{J} = \sum_{n=0}^{\infty} \left(y_n^\top Q y_n + z_n^\top R z_n \right), \quad (21)$$

where $Q \succeq 0$ and $R \succ 0$ are state and control weighting matrices, respectively. The optimal gain K is obtained by solving the discrete-time algebraic Riccati equation[5]. In practice, we compute K using MATLAB's `dlqr` function from the Control Toolbox.

$$P = F^\top P F - F^\top P D (R + D^\top P D)^{-1} D^\top P F + Q. \quad (22)$$

IV. NUMERICAL RESULTS

We present numerical results for a benchmark problem: the parabolic Liouville–Bratu equation, using the same learned surrogate timestepper NO model introduced in [26]. In this work, we focus exclusively on the design and implementation of coarse (i.e. slow subspace based) feedback controllers to stabilize an unstable spatially varying steady-state. For clarity, we adopt an assumed approximation for the controlled NO-timestepper: we do not learn the exact actuator effect from data, nor do we attempt to address model

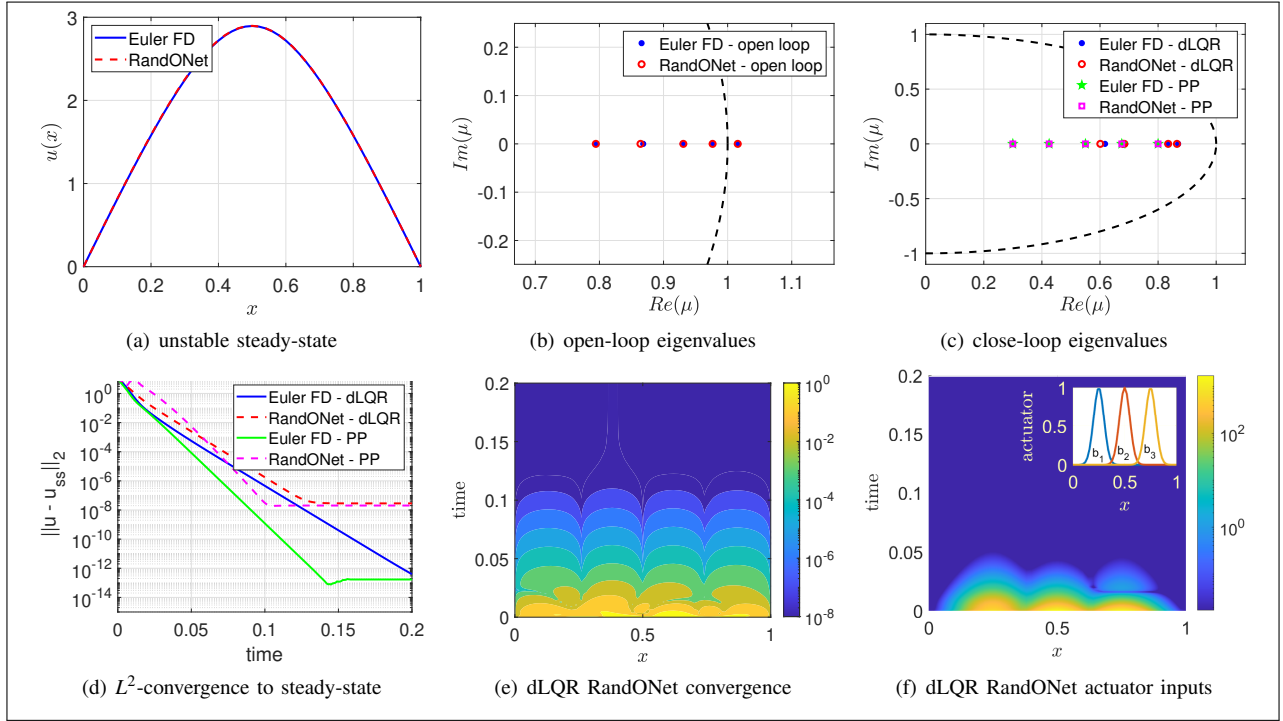


Fig. 2. Equation-free coarse stabilization of an unstable steady-state of the Liouville-Bratu PDE, in Eq.(23), with $\lambda = 2$. We use a RandONet-based NO-timestepper and compare it with an Euler-Finite Difference one, based on the actual PDE. (a) The target unstable steady-state $u_{ss}(x)$. (b) Leading eigenvalues μ_i of the open-loop system’s coarse linearization, computed via Arnoldi iterations. (c) Closed-loop eigenvalues after applying the Pole-Placement (PP) and the dLQR controllers. (d) Convergence of the L^2 -norm error $\|u - u_{ss}\|_2$ for both FD model and RandONet under dLQR and PP control. (e) Spatiotemporal evolution of the controlled state $u(x,t)$ using, indicatively, the RandONet-based dLQR controller. (f) Corresponding absolute amplitude of the spatio-temporal control inputs $|Bz_n|$ of the dLQR controller; in the inset the 3 Gaussian actuators b_1, b_2, b_3 .

uncertainty. That is, for the NO, we treat our approximation as if it were the actual physical system to be controlled. Extensions toward uncertainty mitigation and more accurate representations of the open-loop dynamics can be pursued in subsequent work, without altering the overall framework.

A. The parabolic Liouville–Bratu–Gelfand PDE

We consider the parabolic Liouville–Bratu–Gelfand PDE [33], [45], which models a variety of physical and chemical processes:

$$\frac{\partial u}{\partial t} = \frac{\partial^2 u}{\partial x^2} + \lambda \exp(u) + \mathbf{b}(x) \cdot \mathbf{z}(t), \quad x \in \Omega = [0, 1], \quad (23)$$

where we fix the parameter $\lambda = 2.0$, $\mathbf{z}(t) \in \mathbb{R}^3$ represent the actuator amplitudes and homogeneous Dirichlet boundary conditions $u(0,t) = u(1,t) = 0$ are imposed. In the PDE (23), for actuation, we have considered three spatially localized Gaussian bumps $b_i(x) = \exp(-(x - c_i)^2 / (2\sigma^2))$ with centers $c_i = \{0.25, 0.5, 0.75\}$ and standard deviation $\sigma = 0.05$.

The corresponding autonomous one-dimensional steady-state problem admits an analytical solution [45]:

$$u(x) = 2 \ln \frac{\cosh \theta}{\cosh \theta (1 - 2x)}; \quad \text{with } \cosh \theta = \frac{4\theta}{\sqrt{2\lambda}}. \quad (24)$$

For $0 < \lambda < \lambda_c$, there exist two solution branches that merge at the saddle-node $\lambda_c \sim 3.513830719$, where stability changes; beyond λ_c no steady solutions exist [33], [45].

In [26], we trained the RandONet timestepper models, on autonomous synthetic generated data (PDE solutions), using a $m = 51$ -point spatial discretization for the function input in the branch, and compared the predictions against solutions from a simpler finite-difference/forward Euler scheme, with the same discretization and a 10-times smaller time-step $\Delta t_{FD} = 0.0001$. Full details of the discretization, solver, and dataset structure are provided in [26], where the complete learned NO and the reconstructed bifurcation diagram are reported.

The controlled PDE model. Here, we build on our construction of the learned NO to now perform control tasks. The controller sampling time and the reporting horizon of the neural timestepper are both set to $\Delta t = 0.001$.

In practice, we do not have access to a fully trained controlled (“closed loop”) timestepper $\Phi(u_n, z_n)$ – that form of NO construction is the subject of current research. Instead, we adopt the approximation

$$u_{n+1} \approx \mathcal{S}_{\Delta t}(u_n) + Bz_n, \quad (25)$$

where $B \in \mathbb{R}^{m \times 3}$ encodes the spatial actuator structure. This assumption corresponds to a discrete-time actuation scheme, in which the control input $z(t)$ is held constant over each sampling interval $[0, \Delta t]$ and is applied additively to the state after each autonomous timestep. Equation (25) should be interpreted as a first-order discrete approximation of the continuous-time control action. In continuous time, the exact contribution of the actuators would be represented through a

Duhamel-type integral of the semigroup e^{At} acting on $Bz(t)$. Our formulation amounts to neglecting higher-order terms and retaining the leading-order effect, which is justified here by the small timestep $\Delta t = 0.001$.

To validate our approach, we compare the NO-based controller against a high-fidelity timestepper where the controller is applied directly to the actual PDE. This timestepper employs a finite-difference (FD) scheme with forward Euler integration, using an inner time-step of $\Delta t_{FD} = 0.0001$ within the outer control step of $\Delta t = 0.001$. This provides access to the true controlled timestepper $u_{n+1} = \Phi_{FD}(u_n, z_n)$, where the actuator effects are properly integrated into the dynamics.

For both timesteppers, we design two controllers based on the reduced-order open-loop model (F, D) described in Eq. (18): a discrete-time Linear Quadratic Regulator (dLQR) with weight matrices $Q = 0.5I$ and $R = dt^2 10I$, and a pole-placement controller with desired eigenvalues $\mu_i = [0.30, 0.425, 0.55, 0.675, 0.80]$.

The numerical results are reported in Fig. 2. We compute the unstable steady-state $u_{ss}(x)$ using a Newton-Krylov-GMRES method, as shown in Fig. 2(a). The leading open-loop eigenvalues of the linearized system, computed around u_{ss} via a matrix-free Arnoldi algorithm, are shown in Fig. 2(b). The resulting closed-loop eigenvalues for both the FD-Euler and RandONet models are shown in Fig. 2(c), quantitatively confirming successful stabilization.

Starting from a perturbed initial condition $u_0 = u_{ss} \cdot (1.2 + 0.4 \sin(10\pi x) + 0.4e^x)$, we simulate the closed-loop response. Fig. 2(d) shows the L^2 -norm error $\|u - u_{ss}\|_2$ over time for both controllers and both models. Indicatively, the spatiotemporal evolution of the state under the RandONet-dLQR controller is shown in Fig. 2(e), demonstrating smooth convergence to the target steady-state. The corresponding absolute amplitude control signals $|B(x) \cdot z(t)|$ is shown in Fig. 2(f).

The results show consistent performance between the RandONet-based controllers and the FD-based benchmark. We note that the FD controller achieves a lower final error (near machine precision) because the model is exact. The RandONet controller saturates at an error of $\sim 10^{-7}$, a limitation imposed by the accuracy of the identified NO and the numerical precision of the fixed-point computation. We remark that the RandONet-based controllers were designed and tested under the assumption that the control action is applied in the approximated actuator effect form, and not to the actual physical model. The framework's robustness to plant-model mismatch remains to be investigated in future work.

V. CONCLUSION

In this work, we have revisited the equation-free (EF) framework for the systematic analysis and control of complex systems, addressing a central limitation of the original methodology: its reliance on repeated, potentially expensive, calls to a fine-scale simulator. We have shown that *local neural operator (NOs) surrogates*, trained on spatiotemporal data, can effectively replace the need of a

first-principles-derived microscopic timestepper. This data-driven NO-timestepper seamlessly integrates into established equation-free computational protocols, enabling the matrix-free identification of coarse steady-states, the estimation of their stability through Arnoldi-based eigensolvers, and the subsequent design of low-dimensional, stabilizing controllers. The proposed approach was demonstrated by successfully stabilizing an unstable, spatially structured steady-state of the Liouville-Bratu PDE using both dLQR and pole-placement (PP) techniques designed on a reduced-order model, with performance consistent with a controller derived from the known PDE.

This work illustrates, for the first time, an end-to-end equation-free control pipeline where the only requirement is a dataset of short-horizon simulations, effectively decoupling the framework from the need for an explicit, on-demand microscopic simulator.

An important modeling challenge arises from the fact that rich closed loop data are often unavailable. In such cases, controllers must be designed based on the learned autonomous (possibly perturbed) dynamics alone, and the effect of actuation has to be inferred or approximated. While the underlying PDE evolves in continuous time, the NO surrogate provides only a discrete-time model, forcing us to reconcile controller design at the continuous-time level with its sampled-data implementation.

Looking forward, several challenges and exciting research directions emerge. Beyond the accuracy of the NO surrogate itself, a critical issue is the uncertainty in how actuators affect the dynamics. Future work should therefore incorporate uncertainty quantification not only for model error but also for actuator effects, for example through strategies such as wash-out filters [31], [6]. Extending the framework toward adaptive and model-predictive control, as well as output-feedback settings where the full state is not available, are natural and necessary directions. Ultimately, the real test of this approach will be its application to high-dimensional systems in the presence of experimental data, where first-principles models are unavailable and both open-loop and actuator uncertainties must be actively managed.

REFERENCES

- [1] I. G. Kevrekidis, C. W. Gear, J. M. Hyman, P. G. Kevrekidis, O. Runborg, and C. Theodoropoulos, "Equation-free, coarse-grained multiscale computation: Enabling microscopic simulators to perform system-level analysis," *Communications in Mathematical Sciences*, vol. 1, no. 4, pp. 715–762, 2003.
- [2] G. E. Karniadakis, I. G. Kevrekidis, L. Lu, P. Perdikaris, S. Wang, and L. Yang, "Physics-informed machine learning," *Nature Reviews Physics*, vol. 3, no. 6, pp. 422–440, 2021.
- [3] G. Fabiani, N. Evangelou, T. Cui, J. M. Bello-Rivas, C. P. Martin-Linares, C. Siettos, and I. G. Kevrekidis, "Task-oriented machine learning assisted surrogates for tipping points of agent-based models," *Nature Communications volume*, vol. 15, no. 4117, pp. 1–13, 2024.
- [4] M. Scheffer and S. R. Carpenter, "Catastrophic regime shifts in ecosystems: linking theory to observation," *Trends in ecology & evolution*, vol. 18, no. 12, pp. 648–656, 2003.
- [5] A. Armaou, C. I. Siettos, and I. G. Kevrekidis, "Time-steppers and 'coarse' control of distributed microscopic processes," *International Journal of Robust and Nonlinear Control: IFAC-Affiliated Journal*, vol. 14, no. 2, pp. 89–111, 2004.

- [6] D. G. Patsatzis, L. Russo, I. G. Kevrekidis, and C. Siettos, "Data-driven control of agent-based models: An equation/variable-free machine learning approach," *Journal of Computational Physics*, vol. 478, p. 111953, 2023.
- [7] H. Vargas Alvarez, G. Fabiani, N. Kazantzis, C. Siettos, and I. G. Kevrekidis, "Discrete-time nonlinear feedback linearization via physics-informed machine learning," *Journal of Computational Physics*, vol. 492, p. 112408, 2023.
- [8] P. D. Christofides and J. Chow, "Nonlinear and robust control of pde systems: Methods and applications to transport-reaction processes," *Appl. Mech. Rev.*, vol. 55, no. 2, pp. B29–B30, 2002.
- [9] S. Y. Shvartsman and I. Kevrekidis, "Low-dimensional approximation and control of periodic solutions in spatially extended systems," *Physical Review E*, vol. 58, no. 1, p. 361, 1998.
- [10] I. G. Kevrekidis, C. W. Gear, and G. Hummer, "Equation-free: The computer-aided analysis of complex multiscale systems," *AIChE Journal*, vol. 50, no. 7, pp. 1346–1355, 2004.
- [11] R. Erban, T. A. Frewen, X. Wang, T. C. Elston, R. Coifman, B. Nadler, and I. G. Kevrekidis, "Variable-free exploration of stochastic models: a gene regulatory network example," *The Journal of chemical physics*, vol. 126, no. 15, p. 04B618, 2007.
- [12] C. T. Kelley, *Iterative methods for linear and nonlinear equations*. SIAM, 1995.
- [13] Y. Saad, *Numerical methods for large eigenvalue problems: revised edition*. SIAM, 2011.
- [14] L. Helfmann, N. Djurdjevic Conrad, A. Djurdjevic, S. Winkelmann, and C. Schütte, "From interacting agents to density-based modeling with stochastic pdes," *Communications in Applied Mathematics and Computational Science*, vol. 16, no. 1, pp. 1–32, 2021.
- [15] M. Raissi, "Deep hidden physics models: Deep learning of nonlinear partial differential equations," *The Journal of Machine Learning Research*, vol. 19, no. 1, pp. 932–955, 2018.
- [16] S. Lee, M. Kooshkbaghi, K. Spiliotis, C. I. Siettos, and I. G. Kevrekidis, "Coarse-scale pdes from fine-scale observations via machine learning," *Chaos: An Interdisciplinary Journal of Nonlinear Science*, vol. 30, no. 1, p. 013141, 2020.
- [17] Y. Chen, B. Hosseini, H. Owhadi, and A. M. Stuart, "Solving and learning nonlinear pdes with gaussian processes," *Journal of Computational Physics*, vol. 447, p. 110668, 2021.
- [18] L. Lu, P. Jin, G. Pang, Z. Zhang, and G. E. Karniadakis, "Learning nonlinear operators via deeponet based on the universal approximation theorem of operators," *Nature Machine Intelligence*, vol. 3, no. 3, pp. 218–229, 2021.
- [19] P. R. Vlachas, G. Arampatzis, C. Uhler, and P. Koumoutsakos, "Multiscale simulations of complex systems by learning their effective dynamics," *Nature Machine Intelligence*, vol. 4, no. 4, pp. 359–366, 2022.
- [20] E. Galaris, G. Fabiani, I. Gallos, I. Kevrekidis, and C. Siettos, "Numerical bifurcation analysis of pdes from lattice boltzmann model simulations: a parsimonious machine learning approach," *Journal of Scientific Computing*, vol. 92, no. 2, pp. 1–30, 2022.
- [21] Y. Deng, Z. Hani, and X. Ma, "Hilbert's sixth problem: derivation of fluid equations via boltzmann's kinetic theory," *arXiv preprint arXiv:2503.01800*, 2025.
- [22] Z. Li, N. Kovachki, K. Azizzadenesheli, B. Liu, K. Bhattacharya, A. Stuart, and A. Anandkumar, "Fourier neural operator for parametric partial differential equations," *arXiv preprint arXiv:2010.08895*, 2020.
- [23] Z. Li, N. Kovachki, K. Azizzadenesheli, B. Liu, A. Stuart, K. Bhattacharya, and A. Anandkumar, "Multipole graph neural operator for parametric partial differential equations," *Advances in Neural Information Processing Systems*, vol. 33, pp. 6755–6766, 2020.
- [24] V. Fanaskov and I. V. Oseledets, "Spectral neural operators," in *Doklady Mathematics*, vol. 108, Suppl 2. Springer, 2023, pp. S226–S232.
- [25] G. Fabiani, I. G. Kevrekidis, C. Siettos, and A. N. Yannacopoulos, "Randonets: Shallow networks with random projections for learning linear and nonlinear operators," *Journal of Computational Physics*, vol. 520, p. 113433, 2025.
- [26] G. Fabiani, H. Vandecasteele, S. Goswami, C. Siettos, and I. G. Kevrekidis, "Enabling local neural operators to perform equation-free system-level analysis," *arXiv preprint arXiv:2505.02308*, 2025.
- [27] Z. Li, M. Liu-Schiaffini, N. Kovachki, B. Liu, K. Azizzadenesheli, K. Bhattacharya, A. Stuart, and A. Anandkumar, "Learning dissipative dynamics in chaotic systems," in *Proceedings of the 36th International Conference on Neural Information Processing Systems*, 2022, pp. 16768–16781.
- [28] S. Wang and P. Perdikaris, "Long-time integration of parametric evolution equations with physics-informed deeponets," *Journal of Computational Physics*, vol. 475, p. 111855, 2023.
- [29] C. I. Siettos, M. D. Graham, and I. G. Kevrekidis, "Coarse brownian dynamics for nematic liquid crystals: Bifurcation, projective integration, and control via stochastic simulation," *The Journal of chemical physics*, vol. 118, no. 22, pp. 10149–10156, 2003.
- [30] C. I. Siettos, I. G. Kevrekidis, and N. Kazantzis, "An equation-free approach to nonlinear control: Coarse feedback linearization with pole-placement," *International Journal of Bifurcation and Chaos*, vol. 16, no. 07, pp. 2029–2041, 2006.
- [31] C. Siettos, C. W. Gear, and I. G. Kevrekidis, "An equation-free approach to agent-based computation: Bifurcation analysis and control of stationary states," *EPL (Europhysics Letters)*, vol. 99, no. 4, p. 48007, 2012.
- [32] K. Ogata, *Discrete-time control systems*. Prentice-Hall, Inc., 1995.
- [33] J. P. Boyd, "An analytical and numerical study of the two-dimensional bratu equation," *Journal of Scientific Computing*, vol. 1, pp. 183–206, 1986.
- [34] T. Chen and H. Chen, "Universal approximation to nonlinear operators by neural networks with arbitrary activation functions and its application to dynamical systems," *IEEE Transactions on Neural Networks*, vol. 6, no. 4, pp. 911–917, 1995.
- [35] G. Cybenko, "Approximation by superpositions of a sigmoidal function," *Mathematics of control, signals and systems*, vol. 2, no. 4, pp. 303–314, 1989.
- [36] V. Froese and C. Hertrich, "Training neural networks is np-hard in fixed dimension," *Advances in Neural Information Processing Systems*, vol. 36, pp. 44039–44049, 2023.
- [37] J. Almira, P. Lopez-de Teruel, D. Romero-Lopez, and F. Voigtlaender, "Negative results for approximation using single layer and multilayer feedforward neural networks," *Journal of mathematical analysis and applications*, vol. 494, no. 1, p. 124584, 2021.
- [38] G. Fabiani, "Random projection neural networks of best approximation: Convergence theory and practical applications," *SIAM Journal on Mathematics of Data Science*, vol. 7, no. 2, pp. 385–409, 2025.
- [39] S. Karumuri, L. Graham-Brady, and S. Goswami, "Efficient training of deep neural operator networks via randomized sampling," *arXiv preprint arXiv:2409.13280*, 2024.
- [40] W. B. Johnson, "Extensions of lipschitz mappings into a hilbert space," *Contemp. Math.*, vol. 26, pp. 189–206, 1984.
- [41] B. Igel'nik and Y.-H. Pao, "Stochastic choice of basis functions in adaptive function approximation and the functional-link net," *IEEE Transactions on Neural Networks*, vol. 6, no. 6, pp. 1320–1329, 1995.
- [42] A. Rahimi and B. Recht, "Random features for large-scale kernel machines," *Advances in neural information processing systems*, vol. 20, 2007.
- [43] —, "Uniform approximation of functions with random bases," in *2008 46th annual allerton conference on communication, control, and computing*. IEEE, 2008, pp. 555–561.
- [44] A. N. Gorban, I. Y. Tyukin, D. V. Prokhorov, and K. I. Sofeikov, "Approximation with random bases: Pro et contra," *Information Sciences*, vol. 364, pp. 129–145, 2016.
- [45] G. Fabiani, F. Calabrò, L. Russo, and C. Siettos, "Numerical solution and bifurcation analysis of nonlinear partial differential equations with extreme learning machines," *Journal of Scientific Computing*, vol. 89, no. 2, pp. 1–35, 2021.
- [46] G. Fabiani, E. Galaris, L. Russo, and C. Siettos, "Parsimonious physics-informed random projection neural networks for initial value problems of odes and index-1 daes," *Chaos: An Interdisciplinary Journal of Nonlinear Science*, vol. 33, no. 4, 2023.